J. Astron. Space Sci. 22(2), 89–112 (2005)

HI LINEWIDTHS, ROTATION VELOCITIES AND THE TULLY-FISHER RELATION

Myung-Hyun Rhee[1]† and Adrick H. Broeils[2]

[1]Yonsei University Observatory, Yonsei University, Seoul 120-749, Korea

[2]Kapteyn Astronomical Institute, Groningen, and Origin Nederland B. V., Nieuwegein, The Netherlands

email: rhee@obs.yonsei.ac.kr

(Received April 7, 2005; Accepted April 22, 2005)

ABSTRACT

We determine the rotation velocities of 108 spiral and irregular galaxies (XV-Sample) from first-order rotation curves from position-velocity maps, based on short 21-cm observations with the Westerbork Synthesis Radio Telescope (WSRT). To test the usual random motion corrections, we compare the global HI linewidths and the rotation velocities, obtained from kinematical fits to two-dimensional velocity fields for a sample of 28 galaxies (RC-Sample), and find that the most frequently used correction formulae (Tully & Fouqué 1985) are not very satisfactory. The rotation velocity parameter (the random-motion corrected HI linewidth: W_R^i), derived with these corrections, may be statistically equal to two times the true rotation velocity, but in individual cases the differences can be large. We analyse, for both RC- and XV-Samples, the dependence of the slope of, and scatter in the Tully-Fisher relation on the definition of the rotation velocity parameters. For the RC-Sample, we find that the scatter in the Tully-Fisher relation can be reduced considerably when the rotation velocities derived from rotation curves are used instead of the random-motion corrected global HI linewidths. No such reduction in the scatter is seen for XV-Sample. We conclude that the reduction of the scatter in the Tully-Fisher relation seems to be related to the use of two-dimensional velocity information: accurate rotation velocity and kinematical inclination.

Keywords: galaxies: fundamental parameters, galaxies: kinematics and dynamics, galaxies: spiral, galaxies: distances and redshift, distance scale, radio lines: galaxies

1. INTRODUCTION

The relation between luminosity and rotation velocity, i.e. the Tully-Fisher relation (Tully & Fisher 1977, hereafter TF relation), has been used for many years as a distance indicator. The classical form of this relation relates the inclination-corrected width of the global HI profile to the absolute luminosity of a galaxy. The basic physical interpretation of this empirical correlation is that the profile width gives an estimate of the rotation velocity of a galaxy and, therefore, a measure of the total mass. If the average mass-to-light ratio and surface brightness, or the product of them, is more or less the same for all spirals, then the observed relation follows from the linear correlation

†corresponding author

between the total mass and absolute luminosity (cf. Aaronson et al. 1979, Rhee 1996, 2004a,b). One of the main uncertainties in the application of the TF relation is the transformation of global profile widths to rotation velocities. A relatively small error of 5% in the rotation velocities leads to a distance error of 10%. For this reason, one might expect that the scatter in the TF relation can be reduced (so that the accuracy of distance measurements can be improved) by using rotation velocities measured directly from rotation curves instead of derivatives of profile widths. This principle was first investigated by Rubin et al. (1985) using optical rotation curves of a large sample of spiral galaxies. Recently, this field has attracted new attention due to the availability of better and more sensitive spectrographs, multi-slit spectrographs and imaging Fabry-Pérot spectrometers (e.g. Bothun et al. 1992, Schommer et al. 1993). For the Antlia and Hydra clusters of galaxies Schommer et al. (1993) show that the scatter can be reduced to 0.25 mag by combining optical rotation curves from imaging Fabry-Pérot observations with CCD I-band photometry. Furthermore, as the slope of the TF relation provides constraints on theories of galaxy formation, it is of importance to define 21-cm profile width as close to the true rotation velocity as possible.

In this paper we will use two galaxy samples: The RC-Sample containing 28 galaxies for which HI rotation curves based on 2D velocity fields are available and the XV-Sample consisting of 108 galaxies for which one-dimensional information on the HI distributions along the major axes are available obtained by short 21-cm observations with the Westerbork Synthesis Radio Telescope (WSRT) (see Broeils & van Woerden 1994, hereafter Paper I; Rhee & van Albada 1996, hereafter Paper II; Broeils & Rhee 1997). The general properties of these two samples are described in Sect. 2. We first describe two methods to derive the rotation velocity of a system, which will be used in Sect. 5 for the TF relation. In Sect. 3 we present a method to derive first-order rotation curves for the XV-Sample. We then determine the rotation velocities of the spiral and irregular galaxies (XV-Sample) from these first-order rotation curves.

The usual way to determine rotation velocities for a large number of galaxies is to measure the widths of global HI profiles (mostly with single-dish radio telescopes), and to correct these for inclination. Several investigators (e.g. Bottinelli et al. 1983, hereafter BGPV; Tully & Fouqué 1985, hereafter TFq) have shown that these widths are good indicators of the rotation speeds of galaxies, provided that extra corrections for random gas motions are applied. In Sect. 4 the generally accepted correction formulae are discussed and we investigate how large these corrections have to be. We will show that the size of the random-motions correction is of importance, since it can have significant influence on the slope of and scatter in the TF relation.

In Sect. 5 we show that for a sample of about 28 galaxies with high quality HI rotation curves (RC-Sample) the scatter is reduced by about 20% (0.15 mag) if we use velocities obtained from rotation curves instead of the HI profile widths. This motivated us to analyse the dependence of the slope and scatter of the TF relation of XV-Sample on the definition of the rotation velocity, since also for this sample we have two - more or less - independent determinations of the rotation speeds.

2. DATA

2.1 RC-Sample

From the literature a sample of 28 galaxies with accurate HI rotation curves, measured with either the WSRT or the Very Large Array (VLA), was selected. Most of them are in common with Broeils (1992a) and Rhee (1996). The basic properties for these galaxies are listed in Table ??. Information in Table ?? requiring explanation is given below.

(1) Distances (column 2): We have used Cepheid-based distances when available: 0.84 Mpc for

Table 1. Physical properties of the RC-Sample galaxies.

Name	D	$M_B^{b,i}$	M_H	i_{RC}	W_{20}	W_{50}	V_{max}	i_{max}	W_t^{20}	W_t^{50}	V_{flat}	i_{flat}	W_t^{20}	W_t^{50}	Ref
	Mpc	mag	mag	o	km/s	km/s	km/s	o	km/s	km/s	km/s	o	km/s	km/s	
(1)	(2)	(3)	(4)	(5)	(6)	(7)	(8)	(9)	(10)	(11)	(12)	(13)	(14)	(15)	(16)
D 105	15.7	-17.98		64	155	150	82	64	10	3	82	64	10	3	1
D 154	4.0	-14.78		64	93	95	48	57	25	23	47	57	28	26	2,3
D 168	3.6	-15.77		61	85	62	55	61	<0	<0	54	61	<0	<0	1
D 170	12.0	-15.71		70	134	118	66	70	14	<0	63	70	22	<0	4
I 2574	3.6	-18.03	-17.82	75	122	105	68	75	<0	<0	66	75	<0	<0	5
M 33	0.8	-19.20	-20.63	57	196	185	108	57	17	5	107	57	18	6	6
N 55	1.3	-18.32		77	192	182	87	75	26	15	86	75	28	17	7
N 247	2.8	-18.56	-19.92	74	215	204	108	74	8	<0	106	74	12	<0	8
N 253	3.7	-20.84	-23.60	72	412	408	224	64	9	5	224	64	9	5	9
N 300	2.2	-18.56		55	156	141	97	50	9	<0	90	55	11	<0	10
N 801	79.0	-21.73		75	474	465	222	75	45	36	218	75	53	44	1
N 1560	3.2	-17.19	-18.75	80	156	147	79	80	1	<0	77	80	5	<0	1,11
N 2403	3.5	-19.78	-21.52	60	247	239	136	60	11	3	134	60	15	7	12
N 2460	23.9	-19.95		50	357	323	221	50	18	<0	221	50	18	<0	1
N 2841	12.0	-21.52	-23.65	77	604	590	326	65	13	<0	294	77	31	17	12
N 2903	6.4	-20.36	-22.78	66	380	367	203	66	8	<0	180	66	50	37	12
N 2998	67.4	-21.73		58	399	390	214	58	36	27	209	58	45	36	1
N 3109	1.3	-16.21		70	126	120	67	75	<0	<0	66	70	3	<0	13
N 3198	9.4	-20.11	-21.33	77	319	309	157	72	20	10	149	77	29	19	12
N 5033	11.9	-20.54	-23.04	66	437	421	219	66	36	20	195	66	80	64	12
N 5533	55.8	-21.62		50	450	417	273	50	31	<0	239	50	83	50	1
N 5585	7.6	-18.85	-19.42	52	156	143	92	52	15	<0	91	52	17	1	14
N 6503	4.4	-18.64	-20.56	74	268	250	121	74	36	18	115	74	48	29	12
N 6674	49.3	-21.65		52	449	433	266	54	16	<0	241	53	64	48	1
N 7331	14.9	-21.98	-24.79	75	516	495	242	75	49	28	238	75	57	36	12
N 7793	3.1	-18.36	-19.63	47	183	174	117	47	13	3	105	47	33	22	15
U 2259	9.8	-16.64		41	128	121	90	41	15	4	90	41	15	4	16
U 2885	79.1	-21.68		64	601	571	298	64	65	35	298	64	65	35	17

Notes to Table 1: Sources of the references (column 16)

1 Broeils (1992a) 2 Carignan & Freeman (1985) 3 Carignan & Beaulieu (1989)
4 Lake, Schommer & van Gorkom (1990) 5 Martimbeau & Carignan (1994) 6 Kolkman (1995)
7 Puche, Carignan & Wainscoat (1991) 8 Carignan & Puche (1990b) 9 Puche, Carignan & van Gorkom (1991)
10 Puche, Carignan & Bosma (1990) 11 Broeils (1992b) 12 Begeman (1987)
13 Jobin & Carignan (1990) 14 Côté, Carignan & Sancisi (1991) 15 Carignan & Puche (1990a)
16 Carignan, Sancisi & van Albada (1988) 17 Roelfsema & Allen (1985)

M 33 (Madore & Freedman 1991), 2.15 Mpc for NGC 300 (Freedman et al. 1992), 3.52 Mpc for NGC 2403 (Freedman, Lee, & Madore 1996), and 1.26 Mpc for NGC 3109 (Capaccioli, Piotto, & Bresolin 1992). We have adopted the M 101 group distance of 7.55 Mpc for NGC 5585 (Kelson et al. 1994), the M 81 group distance of 3.63 Mpc for IC 2574 (Freedman et al. 1994), and the Canes Venaticorum I (CVn I) group distance of 4 Mpc for DDO 154 (Carignan & Beaulieu 1989). The distances to the other galaxies have been calculated from the systemic velocity, corrected for the Virgo-centric flow following Kraan-Korteweg (1986), and a Hubble constant of 75 $\mathrm{km\,s^{-1}\ Mpc^{-1}}$.

(2) Absolute magnitudes: $M_B^{b,i}$ (column 3) is the total absolute blue magnitude, corrected for Galactic and internal absorption effects following TFq using the mean kinematical inclination (column 5). The mean kinematical inclinations are taken from the original papers (see column 16 for references). The apparent blue magnitudes are taken from the Lyon-Meudon Extragalactic Database (LEDA). M_H (column 4) is the absolute near-infrared H magnitude (inside one third of the *blue* diameter), not corrected for internal extinction. The apparent magnitudes, already corrected for Galactic extinction, are taken from Tormen & Burstein (1995).

(3) Rotation velocities[3]: W_{20} (column 6) and W_{50} (column 7) are the linewidths measured at 20 and 50% of the peak flux of the global HI profile, respectively, corrected for instrumental

[3]Throughout this paper we use the symbol W for widths not corrected for inclination. A superscript 'i' (i.e. W^i) has been added when the width was corrected. The symbol V denotes different definitions of the rotation velocity, which means that it is always corrected for inclination, unless stated otherwise.

broadening following Bottinelli et al. (1990). The *raw* HI linewidths are determined from HI synthesis observations. $V_{\rm max}$ (column 8) is the maximum rotation velocity, measured beyond two-thirds of the optical radius (R_{25}), to avoid the central peak (which might be due mainly to the bulge) in the rotation curve. $i_{\rm max}$ (column 9) is the kinematical inclination determined at the radius where $V_{\rm max}$ is defined. $V_{\rm flat}$ (column 12) is the rotation velocity determined from the flat, outer part of the HI rotation curve. In case the rotation curve continues to be rising, $V_{\rm flat}$ is an average of the outermost reliable points. $i_{\rm flat}$ (column 13) is the kinematical inclination determined at the radius where $V_{\rm flat}$ is defined.

(4) Random-motion parameters: $W_{\rm t}$ is the random-motion parameter (see Sect. 4). The values of $W_{\rm t,20}$ and $W_{\rm t,50}$ corresponding to $V_{\rm max}$ are listed in columns 10 and 11 and those corresponding to $V_{\rm flat}$ are listed in columns 14 and 15.

2.2 XV-Sample

Our XV-Sample consists of 108 galaxies observed with the WSRT (see Papers I and II). The basic properties for these galaxies are listed in Table **??**. Distances (column,2) and HI linewidths W_{20} and W_{50}, corrected for instrumental broadening following Bottinelli et al. (1990), are taken from Papers I and II. Blue absolute magnitudes $M_{\rm B}^{\rm b,i}$ (column 3) and optical inclinations $i_{\rm opt}$ (column 5) are derived from the LEDA database, using the prescriptions given in Papers I and II. Note that the distances to the galaxies have been calculated from the systemic velocity, corrected for the Virgo-centric flow following Kraan-Korteweg (1986), and a Hubble constant of 75 km s^{-1} Mpc^{-1}. Information in Table **??** requiring further explanation is given below.

(1) Absolute H magnitude: $M_{\rm H}$ (column 4) is the absolute near-infrared H magnitude (inside one third of the *blue* diameter), not corrected for internal extinction. The apparent magnitudes, already corrected for Galactic extinction, are taken from Tormen & Burstein (1995).

(2) Random-motion corrected linewidths: $W_{\rm R,20}$ and $W_{\rm R,50}$ (columns 8 and 9) are HI linewidths corrected the random-motion. Newly determined random-motion parameters ($W_{\rm t,20} = 20$ and $W_{\rm t,50} = 8$ km s^{-1}; see Sect. 4) are used for corrections.

(3) Rotation velocities: $V_{\rm XV}$ (column 10) is the maximum rotation velocity measured from the first-order rotation curves from the position-velocity map (see Sect. 3).

3. ROTATION VELOCITIES

One of the advantages of short WSRT observations (see Papers I and II) over single-dish observations is that one can study the kinematics of neutral hydrogen along the major axis of a galaxy. Short WSRT observations provide one-dimensional information about the kinematics and distribution of the neutral hydrogen gas projected on the so-called resolution axis. The observations of each galaxy were made in such a way that the resolution axis coincides with the major axis of that galaxy, so that a position-velocity map (XV-map) of the HI distribution projected on the major axis was obtained.

In this section we describe how first-order rotation curves are derived from these position-velocity maps given a number of assumptions. From each rotation curve we then determine the velocity ($V_{\rm XV}$) that gives the best representation of the circular velocity in the plane of the galaxy. The method for deriving rotation curves from one-dimensional XV-maps is similar to the way one derives a rotation for an edge-on galaxy (e.g. Sancisi & Allen 1979). The method is based on three assumptions: 1) the gas motions are circular everywhere in the disc; 2) HI can be detected at each point along the major axis; 3) the inclination does not vary significantly with radius. There are, however, major differences. For systems close to edge-on the inclination corrections to convert observed

Table 2. Physical properties of the XV-Sample galaxies.

Name	D	$M_B^{b,i}$	M_H	i_{opt}	W_{20}	W_{50}	$W_{R,20}$	$W_{R,50}$	V_{max}
	Mpc	mag	mag	°	km/s	km/s	km/s	km/s	km/s
(1)	(2)	(3)	(4)	(5)	(6)	(7)	(8)	(9)	(10)
D 77	18.8	-19.39		52	167	151	150	144	84
D 80	30.9	-19.47		63	62	49	55	47	20
D 105	15.7	-17.99		64	154	147	138	140	73
D 165	2.9	-15.20		57	67	44	60	42	14
D 168	3.6	-16.07		76	82	59	73	56	25
D 185	5.0	-16.10		86	102	78	91	74	42
I 167	40.8	-20.12		50	178	139	160	132	81
I 381	37.8	-20.90	-23.04	57	285	269	265	261	151
I 529	35.3	-21.04	-22.30	65	327	302	307	294	151
N 100	13.6	-18.05	-20.04	90	219	209	200	201	98
N 514	34.2	-20.97		35	253	245	233	237	197
N 691	37.3	-21.24		45	346	328	326	320	233
N 697	43.2	-21.42		75	456	432	436	424	206
N 753	67.7	-22.00		37	339	320	319	312	227
N 772	34.6	-22.49	-24.79	58	455	405	435	397	261
N 784	5.7	-17.88	-18.42	79	114	95	102	90	47
N 803	29.5	-20.23	-22.07	67	264	253	244	245	124
N 818	58.8	-21.69		67	441	427	421	419	219
N 918	21.9	-19.38	-21.96	56	262	245	242	237	140
N 949	11.5	-18.76	-20.54	53	201	175	182	167	106
N 1003	11.8	-19.62	-20.67	69	224	212	205	204	110
N 1156	7.6	-18.09		36	103	73	92	70	60
N 1171	39.5	-20.79	-23.19	67	295	282	275	274	126
N 1560	3.2	-17.19	-18.75	90	155	146	139	139	68
N 2268	34.7	-21.52	-23.54	54	378	366	358	358	203
N 2357	32.5	-19.71	-22.47	90	345	324	325	316	148
N 2460	23.9	-19.91		44	357	324	337	316	226
N 2535	56.8	-21.31	-23.00	61	144	118	129	112	41
N 2541	10.7	-18.96	-19.93	65	204	192	185	184	94
N 2683	6.4	-19.90	-22.32	82	434	426	414	418	198
N 2715	20.4	-20.90		74	292	286	272	278	134
N 2742	22.3	-20.46		61	319	303	299	295	155
N 2770	29.6	-20.70	-22.05	77	354	335	334	327	152
N 2976	3.6	-17.92	-19.04	61	145	113	130	107	63
N 2998	67.4	-21.80		64	394	382	374	374	196
N 3027	19.4	-20.07	-20.46	64	223	204	204	196	108
N 3041	21.9	-20.01		51	288	274	268	266	153
N 3254	22.4	-20.42	-22.40	78	424	403	404	395	195
N 3264	17.3	-19.46	-19.14	66	151	129	135	123	58
N 3319	12.4	-19.59	-20.08	57	217	198	198	190	111
N 3338	21.0	-20.84	-22.71	55	342	329	322	321	175
N 3359	18.7	-21.17	-22.28	58	256	241	236	233	139
N 3432	8.8	-19.19	-20.00	79	258	251	238	243	122
N 3486	8.6	-19.29		46	233	209	213	201	149
N 3614	36.0	-20.73		55	302	293	282	285	164
N 3646	59.6	-22.85		58	528	512	508	504	274
N 3666	15.4	-19.35	-21.41	78	273	259	253	251	130
N 3675	13.0	-20.25	-22.95	58	417	407	397	399	232
N 3733	21.1	-19.49	-20.68	66	237	234	217	226	122
N 3756	22.7	-20.52	-22.12	62	295	283	275	275	150
N 3769	13.0	-19.10		77	240	234	220	226	117

Table 2. (continued)

Name	D	$M_B^{b,i}$	M_H	i_{opt}	W_{20}	W_{50}	$W_{R,20}$	$W_{R,50}$	V_{max}
	Mpc	mag	mag	o	km/s	km/s	km/s	km/s	km/s
(1)	(2)	(3)	(4)	(5)	(6)	(7)	(8)	(9)	(10)
N 3877	16.7	-20.51	-22.68	83	360	356	340	348	161
N 3893	17.8	-20.90	-22.60	59	299	266	279	258	149
N 3917	18.0	-19.95	-21.51	83	289	276	269	268	127
N 3949	14.6	-19.98	-21.48	55	277	251	257	243	132
N 3953	19.2	-21.50	-23.61	62	428	408	408	400	216
N 4062	9.6	-18.79	-20.72	66	303	302	283	294	147
N 4068	4.1	-15.59		62	75	55	67	53	28
N 4096	9.4	-19.84	-21.28	80	319	284	299	276	131
N 4100	19.6	-20.64	-22.79	76	401	377	381	369	170
N 4144	4.3	-17.31	-18.11	82	167	155	150	148	79
N 4157	14.2	-19.84	-22.69	90	411	392	391	384	184
N 4183	15.0	-19.21	-20.58	90	242	233	222	225	105
N 4217	18.9	-20.51	-22.86	85	406	387	386	379	187
N 4414	8.7	-19.42	-21.97	56	403	379	383	371	216
N 4534	11.3	-17.75		38	126	117	112	111	86
N 4545	41.7	-20.65	-22.27	57	256	274	236	266	126
N 4559	9.6	-20.40	-21.74	71	249	239	229	231	114
N 4605	4.2	-18.13		69	179	132	161	125	76
N 4814	38.9	-20.80		47	363	332	343	324	196
N 4861	14.3	-17.55		60	110	87	98	83	50
N 5023	6.3	-17.37	-18.50	90	186	176	168	168	82
N 5205	29.2	-19.53	-21.96	57	251	241	231	233	134
N 5350	36.1	-21.10		39	313	290	293	282	215
N 5351	52.6	-21.28		59	425	402	405	394	176
N 5523	18.6	-19.54	-21.19	77	277	268	257	260	128
N 5529	43.3	-21.60	-24.24	90	582	552	562	544	256
N 5533	55.8	-21.68		57	439	409	419	401	236
N 5678	31.2	-21.40		68	410	385	390	377	184
N 5783	36.6	-19.50		53	270	253	250	245	145
N 5879	15.5	-19.75	-21.84	73	281	269	261	261	128
N 5894	38.3	-20.93	-23.24	90	427	410	407	402	187
N 5899	39.7	-21.33		68	483	460	463	452	192
N 5951	27.9	-20.03	-21.40	85	273	262	253	254	121
N 5985	39.2	-21.88		64	533	523	513	515	267
N 6207	16.1	-19.84		68	237	225	217	217	113
N 6236	22.8	-19.40		57	183	165	165	158	87
N 6255	17.1	-18.53	-19.48	67	195	171	176	163	102
N 6339	33.1	-19.75	-21.58	56	224	212	205	204	109
N 6643	25.5	-21.41	-23.16	63	378	344	358	336	158
N 6674	49.3	-21.78		64	437	426	417	418	226
N 6689	11.8	-18.56	-20.10	76	218	205	199	197	91
N 6690	11.8	-18.50	-20.09	74	217	205	198	197	94
N 7177	18.3	-20.21	-22.72	51	300	290	280	282	161
N 7497	25.1	-20.08	-22.48	73	285	255	265	247	128
N 7664	48.7	-20.81		58	339	319	319	311	185
N 7741	13.2	-19.58		47	203	187	184	179	100
N 7753	71.2	-22.00		47	361	320	341	312	208
N 7817	32.9	-21.38	-23.57	80	408	385	388	377	168
U 2855	20.8	-18.59		65	426	406	406	398	200
U 3137	18.3	-17.33	-20.36	90	221	201	202	193	90
U 3580	20.9	-19.64	-21.27	64	234	204	214	196	103

Table 2. (continued)

Name	D	$M_B^{b,i}$	M_H	i_{opt}	W_{20}	W_{50}	$W_{R,20}$	$W_{R,50}$	V_{max}
	Mpc	mag	mag	o	km/s	km/s	km/s	km/s	km/s
(1)	(2)	(3)	(4)	(5)	(6)	(7)	(8)	(9)	(10)
U 5459	19.6	-19.48	-21.23	90	277	262	257	254	132
U 7699	6.5	-16.94	-17.77	78	205	183	186	175	91
U 8146	13.3	-17.26	-18.61	90	168	154	151	147	79
U 11635	68.8	-21.08		69	545	481	525	473	223
U 11651	24.0	-18.53	-21.44	78	269	255	249	247	117
U 11707	15.9	-16.89	-19.49	59	196	183	177	175	103

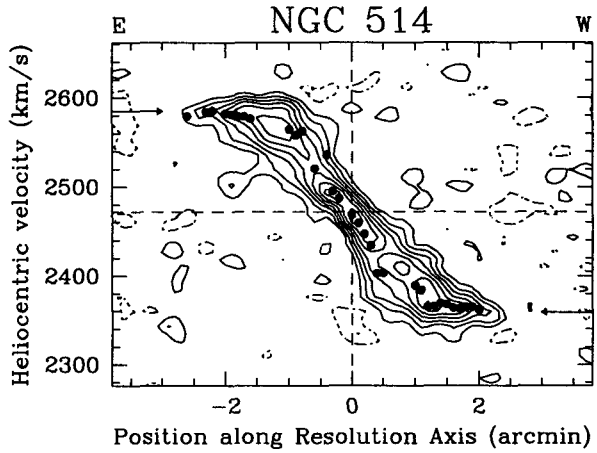

Figure 1. The rotation curve of NGC 514 projected on the position-velocity map of the HI distribution. The horizontal arrows indicate how the representative velocity, V_{XV} (W_{XV}) is defined.

radial velocities to velocities in the plane of the galaxy are negligible, and warps in the HI layer are easily visible (e.g. NGC 4013, Bottema et al. 1987) and hardly change the inclination corrections. For the short observations one can not determine the inclination from the HI distribution or from the kinematics, and a warp in the HI layer would be undetectable. We have to use, therefore, the inclination derived from the observed optical axial ratio and assume that it does not vary with radius.

At each position along the major axis an extreme velocity (i.e. with the large difference with respect to the systemic velocity), to be considered equal to the product $V_{rot} \sin i$, has been defined by decomposing the profile into multiple Gaussian components and taking the central velocity of the most extreme component (cf. Begeman 1987). The result is illustrated in Fig. ??, which displays the rotation curve $V_{rot} \sin i$ vs. X, projected on the position-velocity map of NGC 514. The errors in the *radial* velocities are of the order of $5 - 15$ km s^{-1}, depending on the S/N ratio, the velocity resolution and on the regularity of the HI distribution in space and velocity. The errors in the rotation velocities are of the same order provided the three conditions mentioned above are fulfilled. If, for example, the last condition does not hold (i.e. large variations of inclination with radius are present), then the true circular velocity could differ considerably from the derived V_{rot}. Only with

complete synthesis observations this ambiguity can be removed and reliable rotation curves free from projection effects can be obtained.

Because we are mainly interested in the rotation velocity as one of the quantities to be used in the TF relation, we shall, for each galaxy, only give a *representative* rotation velocity V_{XV} instead of the full rotation curve[4]. Defining such a velocity is not straightforward. One could take the true maximum rotation velocity, V_{max}, or the velocity of the flat, outer part of the rotation curve, V_{flat}. The exact definitions of the representative velocity V_{XV} and the corresponding representative width W_{XV} are of importance, because they have some influence on the slope and dispersion of the TF relation. In the remainder of this paper we define the representative velocity V_{XV} by the true maximum velocity V_{max}, unless it is obvious that this maximum is due to the presence of a bulge component (e.g. NGC 5533, see Paper I) or that it is a local maximum, due to (small-scale) irregularities in the HI distribution (e.g. NGC 5879). The horizontal arrows in the XV-maps of Fig. ?? show the projected maximum rotation velocities for NGC 514. For graphical illustrations of the other 107 galaxies see Figs. A1 of Paper I and Fig. 4 of Paper II. V_{XV} is listed in column 10 of Table ??.

4. CORRECTED LINEWIDTHS

The *classical* way of deriving rotation velocities for a large number of galaxies is to use the width of global HI profiles. Several investigators (e.g. TFq and BGPV) have shown that these widths are good indicators of the rotation velocities, provided that certain corrections are applied. The observed global profile is the result of the combined effects of the rotation and velocity dispersion of the HI gas, and the broadening due to the finite velocity resolution of the receiver. To obtain an estimate of the rotation velocity, the profile has to be corrected for the instrumental broadening and, subsequently, it has to be deconvolved for the effects of broadening due to random motions (Roberts 1978). We have corrected the observed linewidths for instrumental broadening following Bottinelli et al. (1990), according to

$$W_l = W_{l,obs} - F_l(r) = W_{l,obs} + (a \cdot l + b) \cdot r\,, \qquad (1)$$

where W represents a linewidth in km/s and l is the level in percentages ($l = 20$ or 50), r the velocity resolution in km/s and $a(= 0.014)$ and $b(= -0.83)$ are coefficients (see also Papers I & II).

4.1 Random-motion correction

Since the issue of correcting the global profile width for these internal motions was broached (Roberts 1978), several suggestions have been made on how this had to be done. BGPV, for example, assumed that the observed width W_l, corrected for instrumental broadening, could be expressed as $W_l = 2\,(V_{max} \sin i + V_{tur})$, where V_{max} is the maximum circular velocity and V_{tur} is the turbulent velocity in the line-of-sight, due to random motions as well as systematic, non-circular motions, including moderate warps.[5] The value of V_{tur} can be calculated from a model of the velocity dispersions and depends on the level where the width is measured and, if the velocity dispersion is anisotropic, it also depends on the galaxy inclination.

We, however, follow the correction scheme presented by TFq. They argued that, although the linear subtraction of the random motion term gives a good approximation to the corrected pro-

[4]To confuse the reader this velocity was labeled V_{RC} (and the width W_{RC}) in Paper I and V_{max} in Paper II.

[5]Moderate warps can generally be described by circular motions, in another plane than the bulk of the gas in the disc. However, assuming a fixed inclination as is done here, this manifests itself as systematic deviations from circular rotation.

file widths in the case of luminous galaxies with horn-shaped profile, this method fails for low-luminosity galaxies where the random motions become important. The profiles of low-luminosity galaxies often have Gaussian shapes (e.g. NGC 1156 and DDO 80, Fig. A1 of Paper I), due to the combination of a rising rotation curve out to the last measured point and a radial distribution of the HI in the disc with densities increasing towards the center. For this reason, TFq proposed a formula that gives a linear correction for large galaxies, a quadratic correction in the limit of small velocity widths, and a smooth transition for cases between these extremes:

$$\begin{aligned} W^2_{\mathrm{R},l} &= W^2_l + W^2_{\mathrm{t},l}\left[1 - 2\exp(-W^2_l/W^2_{\mathrm{c},l})\right] \\ &- 2W_l W_{\mathrm{t},l}\left[1 - \exp(-W^2_l/W^2_{\mathrm{c},l})\right] . \end{aligned} \tag{2}$$

$W_{\mathrm{R},l}$ denotes the corrected width at level l, W_l is the measured width (corrected for finite velocity resolution), and $W_{\mathrm{c},l}$ and $W_{\mathrm{t},l}$ are, respectively, the characteristic line width and the width due to non-circular motions, as explained below. For widths much larger than $W_{\mathrm{c},l}$, the random motions, $W_{\mathrm{t},l}$, are subtracted linearly from W_l, and for widths much smaller than $W_{\mathrm{c},l}$, $W_{\mathrm{t},l}$ is subtracted quadratically. The characteristic line width $W_{\mathrm{c},l}$ indicates the region where a boxcar profile changes to a Gaussian profile; we adopt a value of 120 km s^{-1} at the 20% level and 100 km s^{-1} at the 50% level, in agreement with TFq and Fouqué et al. (1990; hereafter FBGP).

The most important parameter to be defined is $W_{\mathrm{t},l}$, which represents the broadening of the profile due to random motions. It is related to the velocity dispersion, σ, which is assumed to be isotropic ($\sigma_x = \sigma_y = \sigma_z = 10$ km s^{-1}), and depends on the level of measurement through a factor k_l by the relation $W_{\mathrm{t},l} = 2k_l\,\sigma_z$. For a Gaussian velocity distribution the values of k_l are 1.80 at the 20% level and 1.18 at a level of 50%. However, the distribution of the turbulent velocities need not be Gaussian, consequently k_l may differ from the values given above. Several attempts have been made to optimize the parameter k_l (or $W_{\mathrm{t},l}$) to make the corrected width, $W_{\mathrm{R},l}$, statistically the same as $2V_{\mathrm{rot}}$. For a restricted, well-observed sample of 120 galaxies, BGPV determined the optimum value of $W_{\mathrm{t},l}$ by minimizing the dispersion in the TF relation. They found values of $W_{\mathrm{t},20} = 38$ km s^{-1} and $W_{\mathrm{t},50} = 14$ km s^{-1}, which corresponds to a distribution that has a narrower core and somewhat broader wings than a Gaussian with a dispersion of 10 km s^{-1}. These values were also advocated by TFq and, for example, used in the Nearby Galaxy Catalogue (NBG; Tully 1988).

Another method for optimizing $W_{\mathrm{t},l}$ was used by FBGP. They compared the maximum rotation velocity, derived from the corrected line width $W_{\mathrm{R},l}$ by

$$V_{\max}(\mathrm{LW}) = W^{\mathrm{i}}_{\mathrm{R},l}/2 = W_{\mathrm{R},l}/(2\sin i)\,, \tag{3}$$

with the maximum rotation velocity, $V_{\max}(\mathrm{VF})$, derived from velocity fields obtained by 21-cm interferometric studies. The values obtained for $W_{\mathrm{t},l}$ were 47 km s^{-1} at the 20% level and 27 km s^{-1} at the 50% level, considerably larger than the previous estimates.

We prefer the latter method, since it is a more direct way of finding the optimum value of $W_{\mathrm{t},l}$. However, there were some aspects in FBGP's implementation that motivated us to redo the analysis (see next section). Firstly, FBGP used the compilation by Bosma (1978) of mean rotation velocities that are based on older 21-cm velocity fields, neglecting the work that has been done in this field since that time (e.g. Begeman 1987; Carignan and co-workers, for references see notes to Table ??; Broeils 1992a). Because of the improved quality of the more recent rotation curves the newly derived maximum rotation velocities are preferred. Secondly, the velocities listed by Bosma are average velocities weighted by the HI surface densities in the outer regions of the galaxies, instead of the actual maximum velocities of the rotation curves (in the outer regions), which complicates the analysis. For the sub-sample of Bosma's galaxies that have been re-observed

since 1978, the maximum rotation velocities are on average 20 km s^{-1} larger than the values given by Bosma. Another uncertain aspect of FBGP's analysis is the fact that the sample of 25 galaxies contains 5 galaxies that have inclinations lower than 40°. Begeman (1989) has shown that the rotation curves of such galaxies are unreliable, because effects of varying inclination on the observed velocity field cannot be distinguished from variation in rotation velocity.

4.2 Determination of the random-motion parameter W_t

In this section we try to find the optimum value of W_t, the correction term for the width due to random motions (Eq.(??)), by comparing rotation velocities, obtained from well-determined rotation curves, with the global profile widths, obtained from the same synthesis observations. In doing this, we used the sample of 28 galaxies with accurate HI rotation curves (RC-Sample).

The goal of this exercise is to find the best value of the corrected profile width to be used in the TF relation, which describes the empirical correlation between the total luminosity and the 21-cm global profile width. The basis of this relation is that the profile width gives an estimate of the rotation velocity and therefore provides a measure of the mass which is correlated to the luminosity assuming that spirals on average have the same M/L ratio. Due to the empirical nature of the TF relation, it is not obvious beforehand which point of the rotation curve should be used. Therefore, we determined for each rotation curve two values representing the circular velocity of the gas in the plane of the galaxy: V_{max}, the true maximum rotation velocity (avoiding the central peak), and V_{flat}, the velocity of the flat, outer part of the rotation curve or, if such a part is absent, the average velocity of the outermost reliable points of the rotation curve (see Sect. 3).

For spirals of types Sb and Sc, V_{max} is reached inside the optical radius. If one assumes that the luminous disc determines the maximum value of the rotation curve in this region ("maximum disk hypothesis", cf. van Albada & Sancisi 1986), then the use of V_{max} would provide a natural explanation for the small scatter in the observed TF relation (e.g see Appendix in van Albada et al. 1985). On the other hand, the presence of a prominent bulge could introduce a peak in the inner region of the rotation curve, while the total luminosity could still be dominated by the disc. In such a case the TF relation using the true maximum velocity would predict a larger luminosity than observed. In other words, the precise value of V_{max} is sensitive to small-scale variations in the shape of the rotation curve. (This is also the reason why Bosma (1978) defined the rotation speed by a surface-density weighted, mean velocity.)

This problem can be overcome by using the average velocity of the flat part of the rotation curve. This velocity depends less on the details of the HI distribution and on the presence of irregularities in the rotation curve. For most galaxies, the outer regions are dominated by the dark halo, and hence V_{flat} is set by the halo mass instead of the disc mass. This makes the understanding of the physics behind the TF relation more difficult, although attempts have been made (e.g. Ashman 1990 and references therein; see also Rhee 1996, 2004a,b and references therein).

To derive the widths corresponding to the representative rotation velocities we used the same inclinations that were used in the determinations of the rotation curves:

$$W_{max} = 2V_{max}\ \sin(i_{max}) \quad \text{and} \quad W_{flat} = 2V_{flat}\ \sin(i_{flat}) \tag{4}$$

The widths can therefore be compared directly with the observed widths of global HI profiles at levels of 20% and 50% as determined from the same HI synthesis observations (see Sect. 2 and Table ??).

To see whether there is any systematic differences in linewidth between HI synthesis and single-dish measurements, we have compared these linewidths from HI synthesis observations with those listed in the LEDA. To make a fair comparison, we have used the instrumental broadening

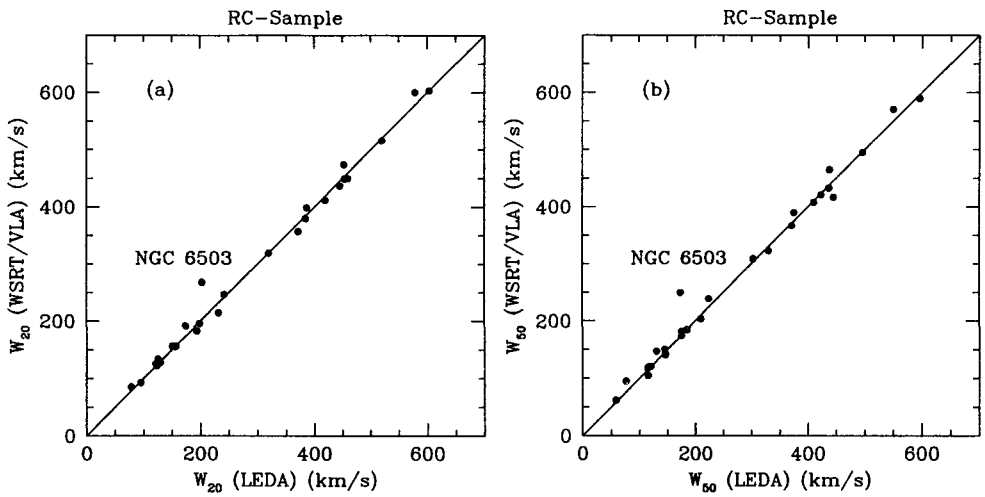

Figure 2. **a** The 20 % HI linewidths measured from HI synthesis observations are plotted against those taken from the LEDA. **b** Same as (**a**) but for the 50 % HI linewidths. The lines indicate equal values.

formula of Bottinelli et al. (1990) (see Eq.(??)), which was adopted in the LEDA. The linewidths of columns 6 and 7 of Table ?? are plotted against those taken from the LEDA in Fig. ??. No obvious discrepant cases were found, except for NGC 6503: the single-dish determinations given in LEDA are wrong for NGC 6503, due to confusion with Galactic HI emission. The mean differences are small: $\langle W_{20}^{\rm Syn} - W_{20}^{\rm LEDA} \rangle = 1 \pm 10$ km s^{-1} and $\langle W_{50}^{\rm Syn} - W_{50}^{\rm LEDA} \rangle = 3 \pm 12$ km s^{-1}.

FBGP determined at each intensity level the best value of $W_{\rm t}$ by minimizing for all galaxies at once, the differences between rotation velocities, obtained from the global profiles, and the maximum rotation velocities as determined by Bosma (1978) from the HI velocity fields. We estimate the value of $W_{\rm t}$ for each galaxy individually, by solving Eq.(??) for $W_{{\rm R},l} = W_{\rm flat}$ or $W_{{\rm R},l} = W_{\rm max}$. In this way a good impression of the range of possible values of $W_{\rm t}$ is obtained. The values of $W_{\rm t,20}$ and $W_{\rm t,50}$ corresponding to $W_{\rm max}$ and $W_{\rm flat}$ are listed in columns 10, 11, 14, and 15 of Table ?? and shown in four histograms in Fig. ??. The average values of all $W_{\rm t}$'s, indicated by the arrows in Fig. ??, are much smaller than the values found by FBGP (which are respectively 47 km s^{-1} and 27 km s^{-1}). For the case that the velocity is defined by $V_{\rm flat}$ the values, $W_{\rm t,20} = 30 \pm 24$ km s^{-1} and $W_{\rm t,50} = 18 \pm 19$ km s^{-1}, are comparable to the values found by BGPV, for the "$V_{\rm max}$" case the random motion parameter is much smaller, $W_{\rm t,20} = 20 \pm 16$ km s^{-1} and $W_{\rm t,50} = 8 \pm 12$ km s^{-1}. Recent work by Verheijen (1997, 2001) shows similiar results.

Figure ?? shows that the range of $W_{\rm t}$ is large. For the width at 50% no correction for random motion is necessary (i.e. $W_{\rm t} \leq 5$) for about 70% of the galaxies, if the representative velocity is defined by $V_{\rm max}$; this percentage is 40 in the "$V_{\rm flat}$" cases. For these galaxies the widths, obtained by projecting the rotation velocities according to Eq.(??), are close to or even larger than the actual widths of the global HI profiles. The latter can be explained by assuming that there is only a small amount of neutral hydrogen present near the radius where the maximum rotation velocity is reached. In some cases the corrections for random motions should even be negative ($W_{\rm t} < 0$), but, using Eq.(??), no formal solution can be found. In Table ?? these events are indicated by '< 0' in columns 10, 11, 14, and 15. Even at the 20% intensity level, $W_{\rm max}$ is larger than the observed profile

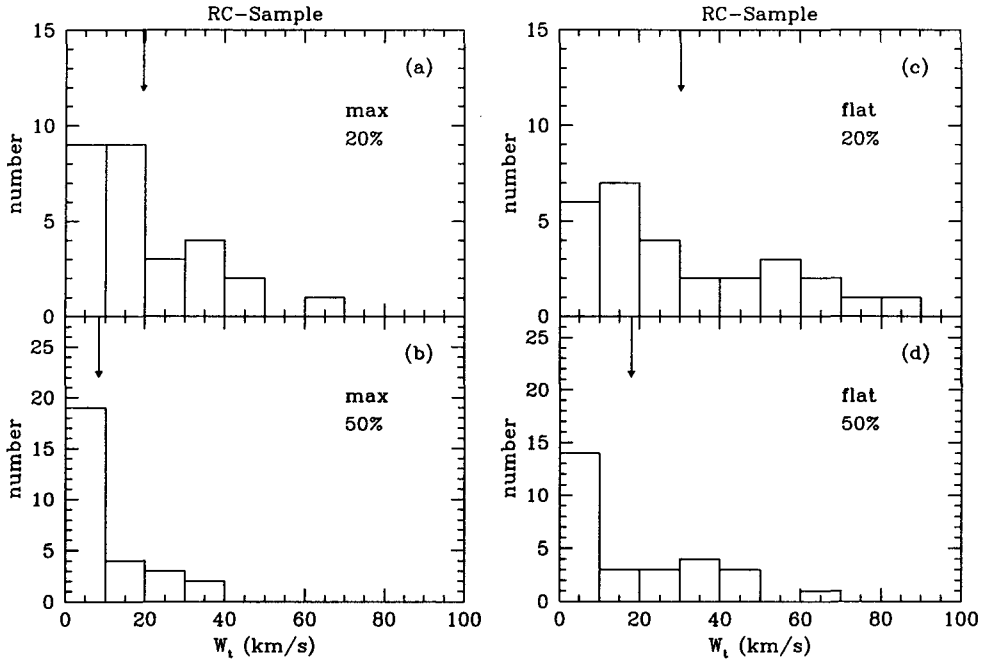

Figure 3. **a** Histogram of the estimated values of W_t for the definition $W_{R,20} = W_{max}$. **b** Same as (**a**) but for $W_{R,50} = W_{max}$. **c** Same as (**a**) but for $W_{R,20} = W_{flat}$. **d** Same as (**a**) but for $W_{R,50} = W_{flat}$. The first bin in each histogram also contains the cases that negative solution was found, because the observed widths of the global profiles are smaller than W_{max} or W_{flat} obtained from the rotation curves.

width (W_{20}) for 3 out of 28 galaxies, and for two galaxies $W_{flat} > W_{20}$. Apparently, also for these cases only a small amount of HI is present at these extreme velocities. In all those cases we used a value of zero in the calculations of the average W_t.

The differences between the average values of W_t for the two definitions of the representative rotation velocity are smaller than their 1σ errors, and provide no basis for choosing one definition instead of the other. However, in many cases only a small amount of neutral gas has velocities close to the true maximum velocity of the rotation curve and consequently this velocity is less-well measurable than the velocity of the bulk of the HI gas, V_{flat}. Hence in general V_{flat} might be preferable. From the above it is clear there is no simple formula to transfer the observed profile widths to rotation velocities, and that the TFq formula (Eq.(2)) has its shortcomings. One can only hope that for a large sample the corrections will on average be correct.

4.3 Comparison of the linewidths and velocities

How do the rotation velocity parameters, calculated from the global HI profiles, compare to the amplitudes of the rotation curves? In Fig. ?? the difference between these two parameters are plotted against W_{20} for the RC-Sample galaxies. Comparing with the maximum amplitude of the rotation curves (Figs. ??a-c) shows first of all that there are zero-point offsets when BGPV's and FBGP's W_t's are adopted. BGPV have overcorrected W_{20} by order of 16 km s^{-1} and FBGP by 24 km s^{-1}. Comparing the random-motion corrected linewidths with $2V_{flat} \sin i$ show smaller discrepancies: BGPV overcorrected W_{20} on average by 5 km s^{-1} and FBGP by 14 km s^{-1} as seen in Figs. ??e

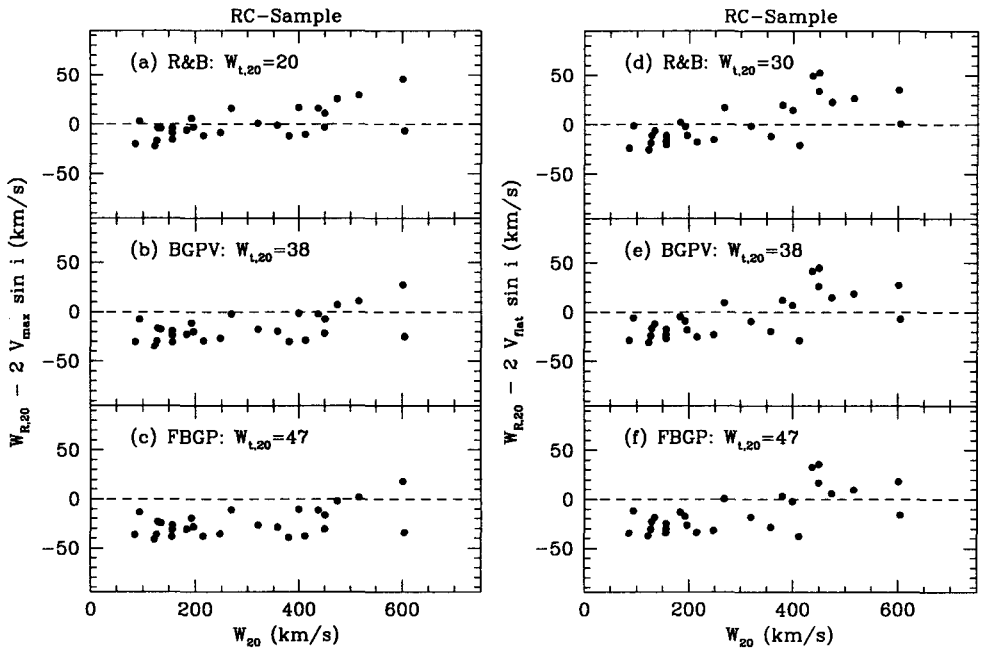

Figure 4. **a** Difference between the random-motion corrected 20% profile width and twice the projected maximum rotation velocity ($2V_{\rm max}\sin i$) as a function of the uncorrected 20% profile width W_{20} for RC-Sample. The random-motion parameter $W_{\rm t,20} = 20$ km s^{-1}, determined in this paper, is used. **b** Same as (**a**) but $W_{\rm t,20} = 38$ km s^{-1} (BGPV) is used. **c** Same as (**a**) but $W_{\rm t,20} = 47$ km s^{-1} (FBGP) is used. **d** Same as (**a**) but twice the projected rotation velocity of the flat part of rotation curve ($2V_{\rm flat}\sin i$) is used instead of $2V_{\rm max}\sin i$. **e** Same as (**d**) but $W_{\rm t,20} = 38$ km s^{-1} (BGPV) is used. **f** Same as (**d**) but $W_{\rm t,20} = 47$ km s^{-1} (FBGP) is used.

and f. These systematic effects disappear when the new $W_{\rm t}$'s, determined in the previous section, are used as seen in Fig. ??a and d. However, 1 σ scatter of 15 km s^{-1} around $\langle W_{\rm R,20} - 2V_{\rm max}\sin i\rangle$ and of 22 km s^{-1} around $\langle W_{\rm R,20} - 2V_{\rm flat}\sin i\rangle$ remains unchanged. This implies that the random-motion corrected linewidths can be easily differ by more than 15 km s^{-1} from the rotation velocities. Figure ?? further indicates that the corrections for large galaxies are too small and for small galaxies they are too large. Two effects could play a role here. For massive galaxies the presence of a bulge component tends to broaden the observed global profile (e.g. NGC 5533), while in the determination of the maximum rotation velocities from the rotation curves the inner, bulge-dominated regions were deliberately avoided. For the dwarf galaxies random motions can be as important as rotation and the rotation curve often keeps increasing out to the edge of the HI distribution, which complicates the definition of the maximum velocity. Similar effects have been found for the case of the 50% profile width.

Now we will apply the new $W_{\rm t}$ values to the XV-sample. In Fig. ?? we plotted the difference between the rotation width parameter ($W_{\rm R}$) and the width from the XV-diagram versus W_{20}. It raises a couple of questions that need to be addressed. First of all, there is a zero-point offset between $W_{\rm R}$ and $W_{\rm XV}$ even though the newly calibrated random-motion parameter $W_{\rm t,20} = 20$ km s^{-1} is used for the random-motion correction: $\langle W_{\rm R,20} - W_{\rm XV}\rangle = 23 \pm 22$ km s^{-1} or 20 ± 17 km s^{-1} after

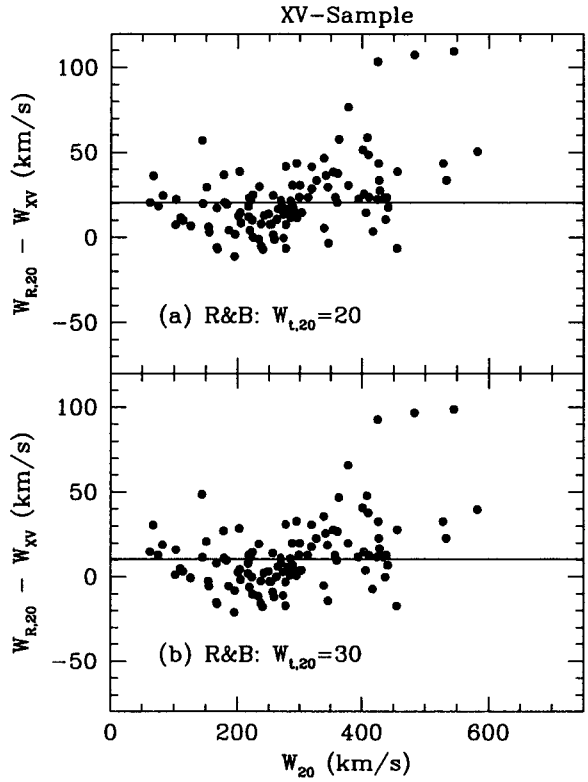

Figure 5. **a** Difference between the random-motion corrected 20% profile width and twice the projected representative rotation velocity ($W_{\rm XV}$), obtained from the XV-maps, as a function of the uncorrected 20% profile width W_{20}. The random-motion parameter $W_{\rm t,20} = 20$ km s^{-1}, determined in this paper, is used. **b** Same as (**a**) but $W_{\rm t,20} = 30$ km s^{-1} is used. The solid lines indicate $\langle W_{\rm R,20} - W_{\rm XV}\rangle$ after rejecting the three extreme outliers.

rejecting the three extreme outliers. The difference is less pronounced when $W_{\rm t} = 30$ km s^{-1}s is adopted: $\langle W_{\rm R,20} - W_{\rm XV}\rangle = 13 \pm 22$ km s^{-1} or 10 ± 17 km s^{-1} after excluding the three extreme outliers.

To investigate what causes this difference, the HI linewidths measured from full HI synthesis observations (RC-Sample) are plotted against those determined from short observations (XV-Sample) for seven galaxies (D 105, D 168, N 1560, N 2460, N 2998, N 5533, and N 6674) in common for RC- and XV-Sample in Fig. ??a. The filled circles represent 50% linewidths and the open circles 20% linewidths. A small systematic effect is seen in the sense that the linewidths from full HI synthesis observations are larger than those from short observations for galaxies with large linewidths. The mean differences between linewidths are small: $\langle W_{20}({\rm full}) - W_{20}({\rm short})\rangle = 5 \pm 5$ km s^{-1} and $\langle W_{50}({\rm full}) - W_{50}({\rm short})\rangle = 4 \pm 4$ km s^{-1}. The differences in linewidth between the HI synthesis observations and single-dish observations (represented by LEDA) are also small (see Paper I and II; see also Sect. 4). Therefore, the offset seen in Fig. ?? must be caused by the systematic differences in the maximum rotation velocity between the full and short HI synthesis observations as shown in Fig. ??b. The average difference is $\langle 2V_{\rm max} \sin i({\rm full}) - 2V_{\rm max} \sin i({\rm short})\rangle = 24 \pm 12$ km s^{-1}

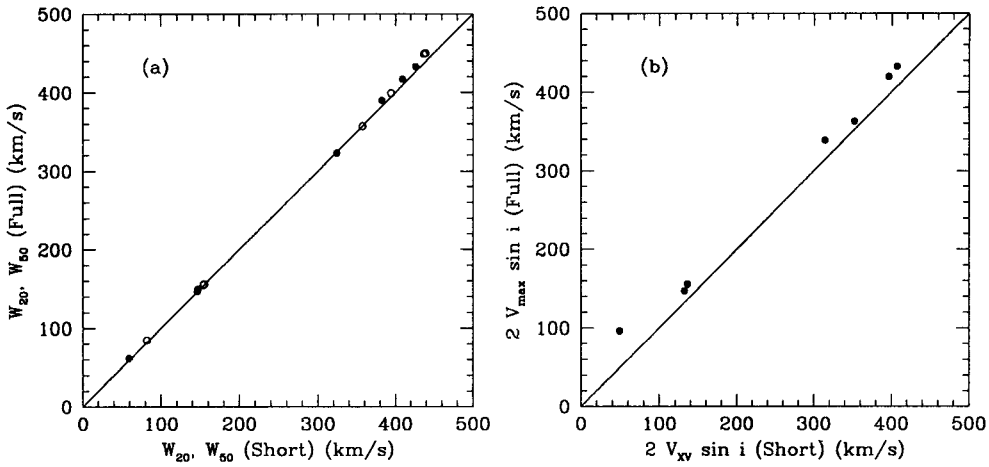

Figure 6. **a** The 20 and 50% HI linewidths measured from full HI synthesis observations (RC-Sample) are plotted against those determined from short observations (XV-Sample) for seven galaxies in common for RC- and XV-Samples. The filled circles represent 50% linewidths and the open circles 20% linewidths. **b** Same as (**a**) but the projected maximum rotation velocities are compared. The solid lines indicate equal values.

or 20 ± 6 km s^{-1} excluding the most deviating point. This can be easily explained by the offset seen in Fig. ??. Part of this 9% (for seven galaxies considered) systematic effect in the maximum velocity can be explained by the different ways the velocities are determined for the one- and the two-(spatial) dimensional observations. With the 1-D observations all HI is projected on the major axis and the velocity profiles are therefore generally broader than those of the 2-D observations. It is likely that the Gaussian decomposition method does not fully correct for this effect. Additionally, the assumptions made in Sect. 3 to derive the representative (maximum) rotation velocity could be violated, i.e. discrepancy between true kinematic position angle of a galaxy and resolution axis of short observations, and inclination variations with radius within a galaxy. A similar systematic effect of order 5-10% is also seen in the optical long-slit observations compared to those with the Fabry-Pérot imaging, most likely due to the uncertainty in the determination of the position angle and due to the skewness of the major axis of a galaxy (e.g. Schommer et al. 1993).

Figure ?? also shows that the differences between $W_{\rm R}$ and $W_{\rm XV}$ for XV-Sample are somewhat larger than those for RC-Sample. In the notes in Appendix A of Paper I some explanations are given how in individual cases large discrepancies between $W_{\rm R}$ and $W_{\rm XV}$ can occur. In principle, we would expect the widths measured directly from the XV-maps to be more reliable than those calculated from the global profiles, since the regions, where the $W_{\rm XV}$'s are determined, were carefully selected.

In Fig. ?? the differences between the widths at 20% and 50% are plotted as a function of the width at 20% intensity level. Fig. ??a shows how much larger the uncorrected 20% width is than the 50% width. In Fig. ??b–d we show how the TFq correction formulae with various values of $W_{\rm t}$ decrease this gap to values close to zero ($\langle \Delta W_{\rm R} \rangle = 4, -7$ and -4 km s^{-1}, for R&B (this paper), BGPV and FBGP, respectively, with standard deviations of about 8 km s^{-1}), although the BGPV and FBGP sets of random-motions parameters still have systematic offsets from zero.

Again these results indicate that the corrections given by Eq.(??) are far from perfect and that it is difficult to judge how accurate the rotation velocities derived from global HI profile widths are.

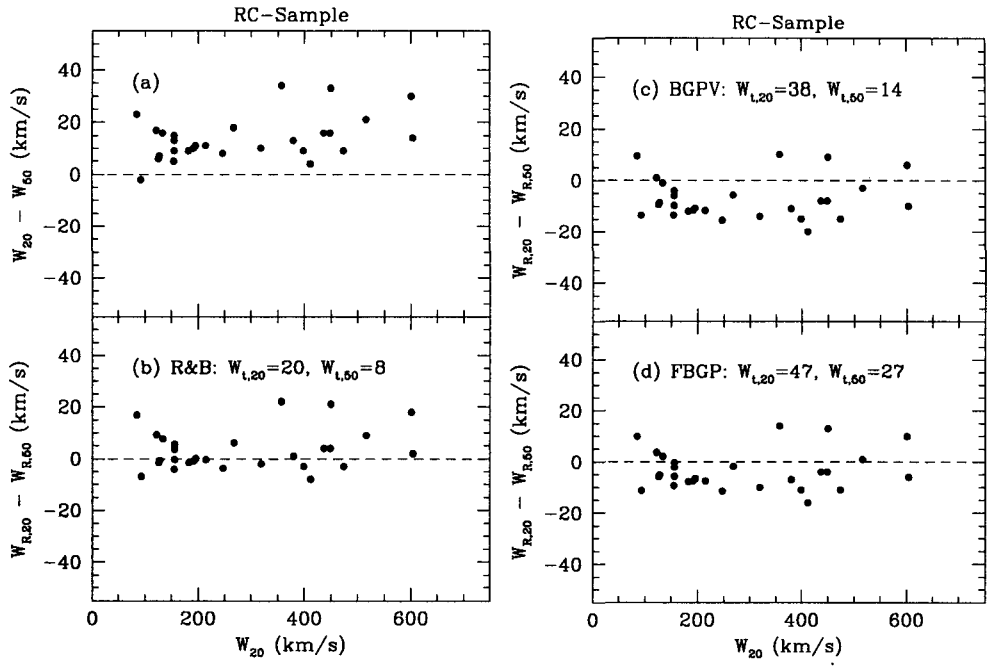

Figure 7. **a** Difference between the uncorrected linewidths at the 20 and 50% levels. **b** Difference of the linewidths at the 20 and 50% levels, corrected for random motions using $W_{t,20} = 20$ and $W_{t,50} = 8$. **c** Same as (**b**) but $W_{t,20} = 38$ and $W_{t,50} = 14$ (BGPV) are used for the random-motion correction. **d** Same as (**b**) but $W_{t,20} = 47$ and $W_{t,50} = 27$ (FBGP) are used for the random-motion correction.

The large spread in the values of W_t indicates that corrections given by Eq.(??) are not as accurate as one would like. Large discrepancies between the corrected widths determined from global profiles and from rotation curves are likely to occur. However, it is clear that the W_t values used by BGPV and FBGP are too large.

5. THE TULLY-FISHER RELATION

During the last decade, astronomers have tried to decrease the dispersion in the TF relation in order to be able to use it as an accurate distance indicator. This has been done by investigating the corrections needed to obtain the fundamental parameters (e.g. TFq and FBGP), by investigating biases due to selection effects (e.g. Giraud 1986), or by using new techniques, like multicolour CCD photometry (e.g. Pierce & Tully 1988), or by using 2D velocity fields (e.g. Schommer et al. 1993, Verheijen 2001). The samples used involve mainly well-defined groups of galaxies, for example clusters, so that the distances to the individual galaxies are the same.

The galaxies in our samples do not form homogeneous groups, neither do they belong to one or more clusters. Each galaxy has an individual distance estimate, either based on its recession velocity or based on the Cepheid P-L relation when available. The reasons for discussing the TF relation for this sample are two-fold: Firstly, we want to see what the influence of the random-motion corrections is on the dispersion and slope of the relation. Secondly, we want to investigate

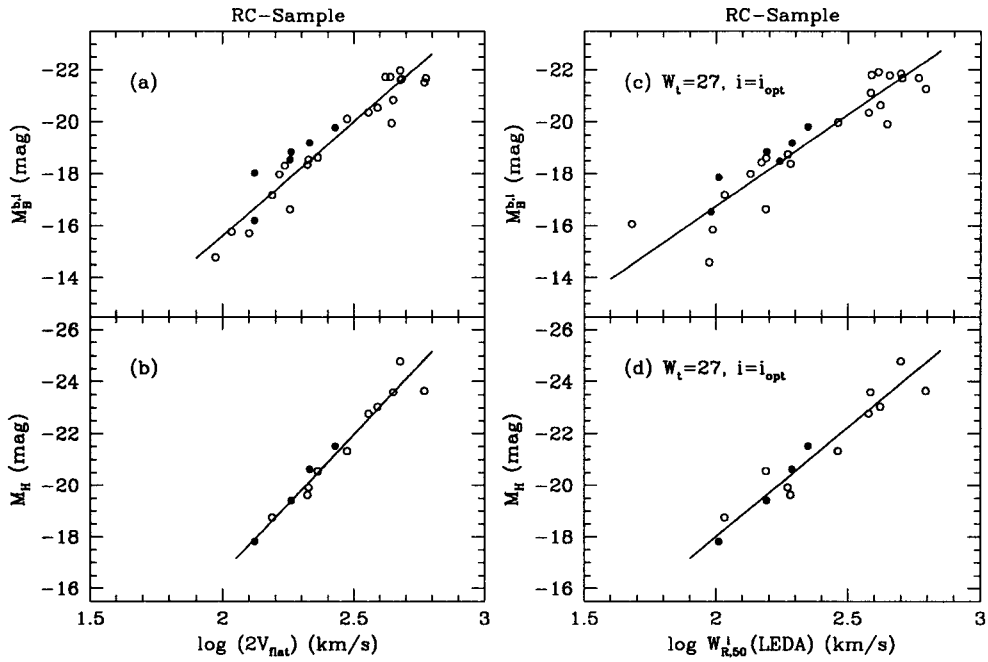

Figure 8. **a** The B-band Tully-Fisher relation for RC-Sample, using the velocities of the flat parts of the rotation curves. The kinematical inclination is used for internal extinction correction to the blue magnitude. **b** Same as (**a**) but for the H-band. **c** Same as (**a**) but using the random-motion corrected 50% linewidths, with $W_{t,50}$ = 27 km s^{-1} (FBGP). The uncorrected linewidths are taken from the LEDA. The optical inclination is used for internal extinction correction to the blue magnitude. **d** Same as (**c**) but for H-band. The filled and open circles represent galaxies with and without Cepheid-based distances, respectively (see Sect. 2). The solid lines indicate the results of the least-squares fits to the data points.

whether the luminosity dispersion in the TF relation can be reduced by using the representative velocity (V_{XV}) or velocity width (W_{XV}), obtained from the rotation curves, instead of the rotation width parameter W_R.

5.1 The Tully-Fisher relation for RC-Sample

In Fig. ?? four versions of the TF relation for RC-Sample are presented; each version has a different definition for the rotation velocity or magnitude. Figures ??a and b show the TF relations using the velocities obtained from the flat parts of the 21-cm rotation curves for the B- and H-band. The kinematic inclination is used for the internal extinction correction to the blue magnitude. In Figs. ??c and d, the 50% HI profile widths, taken from the LEDA and corrected for random motions using Eq.(??) with the FBGP value of $W_{t,50}$ = 27 km s^{-1}, are used with the blue and near infrared magnitudes. The optical inclination is used for the internal extinction correction to the blue magnitude, and to obtain inclination corrected profile width. The filled and open circles represent galaxies with and without Cepheid-based distances, respectively (see Sect. 2). The solid lines indicate the results of the least-squares fits to the data points.

Figure ?? shows that the slopes of the 'V_{flat}' TF relations of Figs. ??a and b are significantly steeper than those for the 'linewidth' TF relations of Fig. ??c and d. The slopes change from $-8.8 \pm$

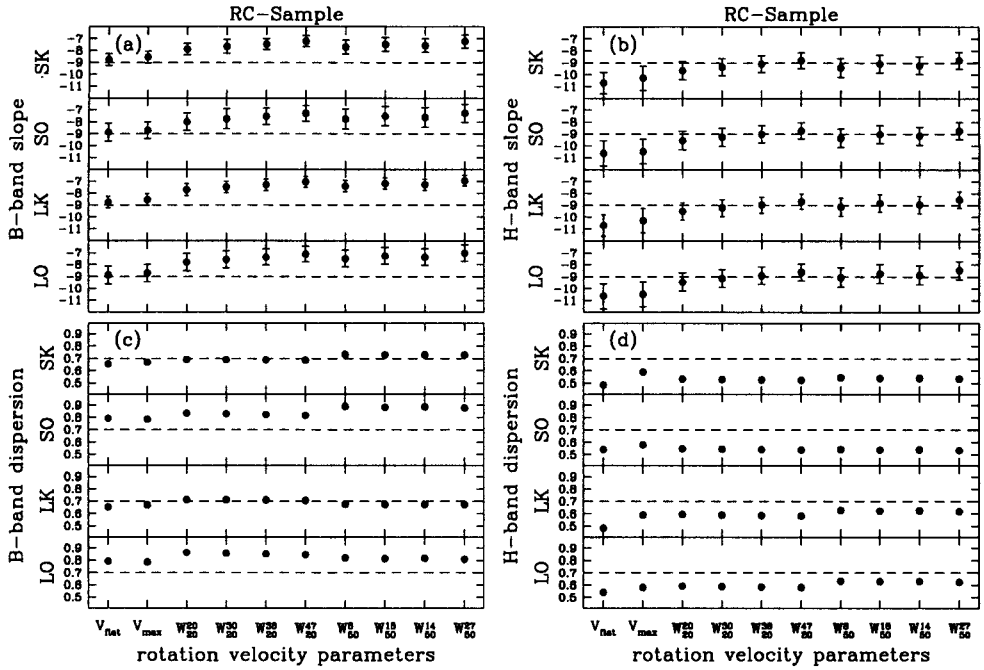

Figure 9. **a** and **b** Slopes of the different versions of the Tully-Fisher relation are plotted. The error bars indicate standard deviations of the slope determination. The symbol 'SK' in the vertical axis denotes that the linewidths are taken from the HI Synthesis observations and that the Kinematical inclinations are used for linewidth correction and for internal extinction correction to the blue magnitude. In the same way, 'SO' denotes use of 'Synthesis' linewidth and 'Optical' inclination, and 'LK' use of 'LEDA' linewidth and 'Kinematical' inclination. And 'LO' denotes use of 'LEDA' linewidth and 'Optical' inclination. The far-left labels in the vertical axis indicate which wavebands are used. On the horizontal axis, ten different definitions for the rotation velocity parameters are used. $V_{\rm flat}$ and $V_{\rm max}$ have the same meaning as used in the text, i.e. the rotation velocity of the flat parts of rotation curve and the maximum rotation velocity. The subscripts in the linewidth symbol 'W' indicates the levels where the linewidths are measured as used in the text. The superscripts in 'W' indicate the values of the random-motion parameters $W_{\rm t}$. **c** and **d** Same as the upper panels but $1\,\sigma$ scatters in the Tully-Fisher relations are plotted.

0.5 to -7.0 ± 0.7 for the B-band and from -10.7 ± 0.9 to -8.5 ± 0.7 for the H-band TF relation. The other interesting aspect of this comparison is the reduction of the scatter in the relations: from 0.81 to 0.66 mag in the B-band and from 0.62 to 0.49 mag in the H-band, between the 'linewidth' and '$V_{\rm flat}$' TF relations. For this sample, the use of the accurate rotation velocity from the rotation curve and the kinematical inclination yields about 0.14 mag reduction of the scatter in the TF relation.

To investigate how the slope and scatter change systematically with different definitions of the TF relation, we have performed least-squares fits to eighty versions of the TF relation, using different combinations of the magnitude and velocity parameters. The results are presented in Fig. ??. The slopes of the different versions of the TF relation are plotted in Fig. ??a and 9b and the panel c & d show the 1 σ scatter in the TF relations.

The symbols in Fig. ?? requiring explanation are given below. The letter 'S' stands for 'Synthesis' linewidth and 'L' for 'LEDA' linewidth. The letter 'K' stands for 'Kinematical' inclination and

'O' for 'Optical' inclination. The symbol 'SK', a combination of 'S' and 'K', in the vertical axis denotes that the linewidths are taken from the HI synthesis observations and the kinematical inclinations are used for linewidth correction and for internal extinction correction to the blue magnitude. The far-left labels in the vertical axis indicate where H and B-band magnitudes are used. In the horizontal axis, ten different definitions for the rotation velocity parameters are given. $V_{\rm flat}$ and $V_{\rm max}$ denote the rotation velocity of the flat part of the rotation curve and the maximum rotation velocity, respectively. The subscripts in the linewidth symbol 'W' indicate the levels where the linewidths are measured. The superscripts in 'W' indicate the values of the random-motion parameters $W_{\rm t}$.

Figure ?? shows first of all that slopes of the TF relation do not change much with the choice of different inclinations and linewidths when only one particular type of the rotation velocity parameter is considered. However, the slope of the TF relation does clearly depend on the wavelength used to measure the optical luminosities. The slope also varies substantially depending on the definition of the velocity parameter. It becomes significantly shallower when the random-motion corrected linewidth are used instead of the rotation velocities from the rotation curves. Use of newly determined $W_{\rm t}$'s from this paper (see Sect. 4) produces the steepest TF slope among the 'linewidth' TF relations, followed by those of BGPV and FBGP. In general, use of the 20%, instead of 50%, linewidths for the TF relation gives a steeper slope.

Unlike the slope, the scatter in the TF relation does vary with the choice of the inclinations and uncorrected linewidths as seen in Fig. ??. Let us consider B-band first. The '$V_{\rm max}$' and '$V_{\rm flat}$' TF relations show the lowest dispersions and the use of the kinematical inclinations instead of the optical ones generally also results in smaller scatter. The reduction of the scatter is about 0.13 mag. When the velocities are defined by the linewidths, the situation is somewhat different, depending on the level where the linewidths are measured. When the 20% linewidths from the synthesis observations are used instead of the LEDA 20% linewidths, the scatters in the TF relations show slight reduction. However in case of the 50% linewidths, the scatters in the TF relations are even slightly increased when the synthesis linewidths are used instead of the LEDA linewidths. It is unclear at this stage what cause this systematic difference. On the whole, the choice of the linewidths does not make a big difference in the scatter in the TF relation.

In the H-band, the '$V_{\rm flat}$' TF relation shows the lowest dispersion whereas the '$V_{\rm max}$' TF relation shows even slightly larger scatter than the 'linewidth' TF relations. The choice of the kinematical inclinations over optical inclinations does not yield a significant reduction in the scatter in the TF relation unlike the behaviour in the B-band. This suggests that kinematical inclinations are mainly important for magnitude corrections for the bluer wavelength bands, not for the conversion of line-of-sight velocities to rotation velocities. On the other hand, the use of the synthesis linewidths instead of the LEDA linewidths gives some improvement, on average 0.06 mag reduction of the scatter in the TF relation. This trend is clearly seen in Fig. ??.

However, dwarf galaxies are often not included in H-band TF relation work because for them the H-band magnitudes are generally not available. Also the most massive galaxies in the RC-sample lack H-band magnitudes (see Table ??). Therefore, it may be possible that the scatter reduction seen in the B-band TF relation is related to the reduction of the number of galaxies used. In fact, the choice of the kinematical inclinations over optical inclinations does not yield significant reduction in the scatter in the B-band TF relation when only the same (14) galaxies as in the H-band are considered. It is therefore difficult to make firm conclusions about the scatter reduction in the B-band TF relation. Note, however, that the $V_{\rm flat}$ and $V_{\rm max}$ TF relations again display the lowest dispersions.

In conclusion, the scatter in the TF relation is reduced by about 0.10 to 0.15 mag if the velocities and kinematical inclinations derived from two-dimensional velocity fields are used instead of the

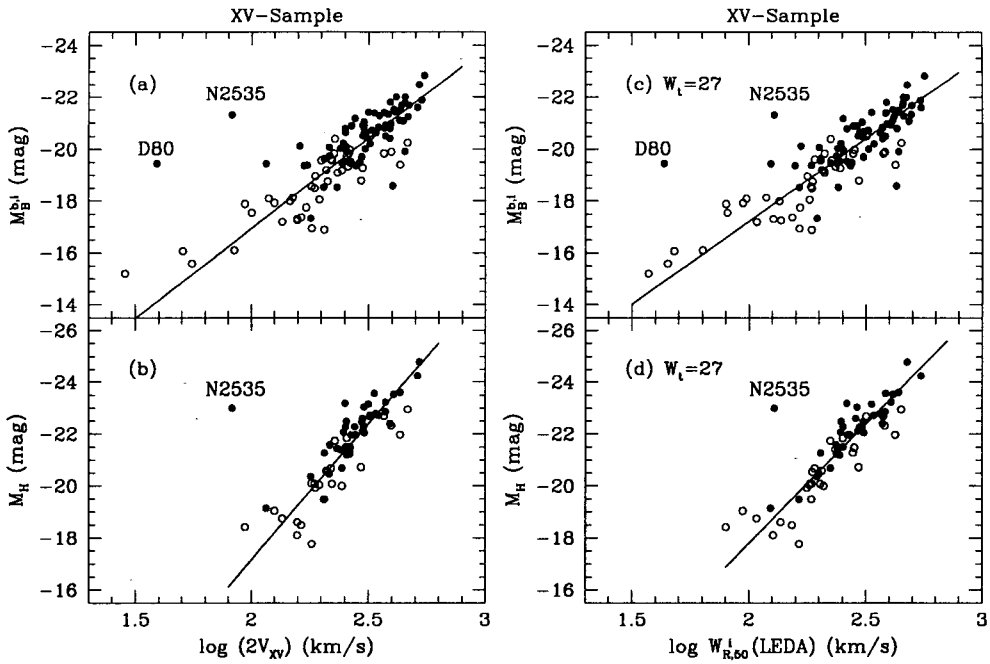

Figure 10. **a** The B-band Tully-Fisher relation for XV-Sample, using the maximum velocities determined from the one-dimensional rotation curves (XV-maps). **b** Same as (**a**) but for the H-band. **c** Same as (**a**) but using the random-motion corrected 50% linewidths, with $W_{t,50} = 27$ km s^{-1} (FBGP). The uncorrected linewidths are taken from the LEDA. **d** Same as (**c**) but for H-band. The filled (open) circles represent galaxies that have a distance larger (less) than 17 Mpc. The solid lines indicate the results of the least-squares fits to the data points except two extreme outliers, indicated by their names.

global HI linewidths and optical inclinations. The above results suggest that one might be able to reduce the observed scatter in the TF relations by fitting a kinematical disc model (like a tilted-ring model, see Begeman 1989) to the velocity fields of galaxies in the samples. This conclusion is confirmed by a recent study of the Hydra and Antlia clusters by Schommer et al. (1993). They combined I-band CCD photometry with imaging Fabry-Pérot observations to obtain two-dimensional optical velocity fields and formed a TF relation with a scatter of about 0.25 mag.

5.2 The Tully-Fisher relation for XV-Sample

In this section we present the TF relation for the galaxies in XV-Sample, for which maximum rotation velocities are also available from the one-dimensional rotation curves (XV-maps). In Fig. ??, the B- and H-band TF relations using the rotation velocities obtained from the XV-maps are compared to those defined by the 50% HI profile widths, taken from the LEDA and corrected for random motions using Eq.(??) with the FBGP value of $W_{t,50} = 27$ km s^{-1}. The solid lines indicate the results of the least-squares fits to the data points, excluding the data point for DDO 80 and NGC 2535, which clearly deviate from the mean relation. The large discrepancy of DDO 80 from the average regression line is hard to explain (see Broeils 1992a for an extensive discussion). The most likely explanation is to be found in a large error in the rotation velocity, since the determination of the total mass $M_{\rm tot}$ has to be wrong by an order of magnitude given the fact that the derived ratio $M_{\rm HI}/M_{\rm tot}$

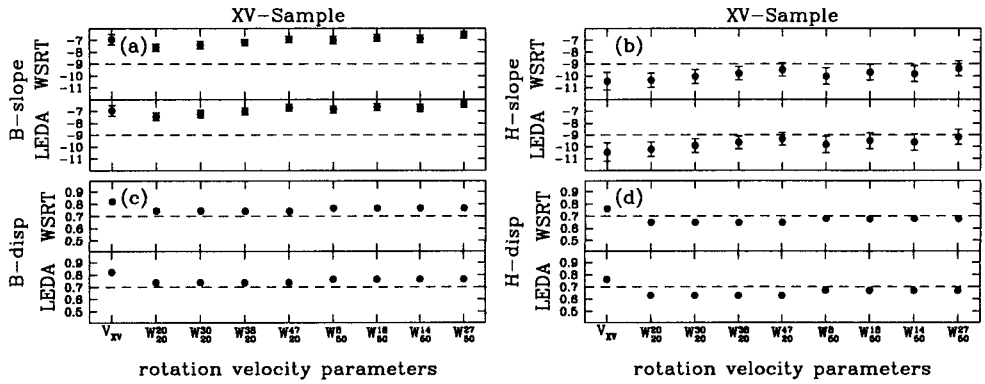

Figure 11. **a** and **b** The slopes of the different versions of the Tully-Fisher relation are plotted. The error bars indicate standard deviations of the slope determination. The symbol 'WSRT' in the vertical axis denotes that the linewidths are taken from the short WSRT HI synthesis observations. And 'LEDA' denotes use of LEDA linewidths. The far-left labels in the vertical axis indicate which wavebands are used. On the horizontal axis, ten different definitions for the rotation velocity parameters are used. $V_{\rm max}$ indicates the maximum rotation velocity from the XV-maps. The subscripts in the linewidth symbol 'W' indicates the levels where the linewidths are measured as used in the text. The superscripts in 'W' indicate the values of the random-motion parameters $W_{\rm t}$. **c** and **d** Same as the upper panels but 1 σ scatters in the Tully-Fisher relations are plotted.

(see Table 1 of Broeils & Rhee 1997) is greater [6] than 2. Also NGC 2535 has an $M_{\rm HI}/M_{\rm tot}$ ratio larger than 1.

Figure **??** shows first of all that there is no real difference between the two TF relations when compared for the same wavebands. The slopes change from -6.4 ± 0.3 to -6.9 ± 0.4 for the B-band and from -9.2 ± 0.6 to -10.5 ± 0.8 for the H-band TF relation, when rotation velocities instead of linewidths are used. The scatter is even increased from 0.77 to 0.82 mag in the B-band and from 0.67 to 0.76 mag in the H-band. Apparently, use of the rotation velocity from the one-dimensional rotation curve does not reduce the scatter in the TF relation.

A comparison using only the distant galaxies, represented by the filled circles in Fig. **??** (distance greater than 17 Mpc), does not change the conclusion: the scatter is reduced somewhat but by nearly the same amount for the 'XV' and the 'linewidth' TF relations. The use of the so-called dynamical profile $W^{\rm i}_{\rm D}$, suggested by TFq for taking into account the velocity dispersion internal to a galaxy, instead of $W^{\rm i}_{\rm R}$ does not change the observed dispersion by a significant amount either.

As a next step, we have performed least-squares fits to 36 different versions of the TF relations similar to what we did in the previous section. Figure **??** shows that the slopes of the TF relation do not change much with the choice of different uncorrected linewidths. The wavelength dependence of the slope of the TF relation is seen here as well. In general, use of the 20%, instead of 50%, linewidths for the TF relation gives a slightly steeper slope. The use of newly determined $W_{\rm t}$'s from this paper (see Sect. 4) produces the steepest TF slope among the 'linewidth' TF relations, followed by BGPV and FBGP, largely confirming the previous results for RC-Sample. While the slopes of the H-band 'XV' TF relations are comparable with those of the '$V_{\rm max}$' TF relation of RC-Sample, the slopes in the B-band are considerably shallower than those of the '$V_{\rm max}$' TF relation of RC-Sample.

[6] Note that the ratio $M_{\rm HI}/M_{\rm tot}$ is proportional to distance, so that a large overestimate of the distance might have the same effect.

This is related to the lack of H-magnitudes for the dwarf galaxies since these galaxies might suffer more from the systematic effects in the maximum rotation velocity measurements between the full and short synthesis observations as found in Sect. 4. In general, the slopes of the TF relations in XV-Sample are somewhat shallower than those found for RC-Sample. Figure ??c and 9d show that the use of the linewidths determined from the short WSRT HI observations instead of the LEDA linewidths does not change the observed dispersion by a significant amount. The use of the rotation velocities from XV-maps even increases the scatter.

In summary, the scatter in the TF relation is not reduced when the rotation velocities from one-dimensional rotation curves are used instead of the global linewidths.

5.3 The Tully-Fisher relation and the definition of the rotation velocity parameters

It has been shown (e.g. Pierce & Tully 1988 and FBGP, Verheijen 2001) that the slope of the TF relation depends not only on the wavelength regime used, but also on the way the profile widths are determined. Recently, Giovanelli et al. (1995) showed that the slope of the TF relation also depends on the internal extinction correction methods to the magnitudes.

As argued before, one might expect the luminosities to correlate more tightly with the rotation velocities obtained directly from the XV-maps, than with the random-motion corrected profile widths. However, this expectation is not fulfilled as seen in Fig. ??. This is also the case if we leave out the most nearby galaxies, for which deviations from the smooth Hubble flow might be a problem. Apparently, the accuracy with which the rotation velocities can be determined from the XV-maps is so much poorer than the determination from two-dimensional velocity fields, that the TF relation for XV-Sample does not become tighter by using $W_{\rm XV}$, in contrast to the results obtained for RC-Sample. This confirms our earlier suggestion that the most important improvement in the velocity parameter of the TF relation can be made by obtaining kinematical inclinations and rotation curves from tilted-ring model analyses of velocity fields. The explanation for this difference is related to the different ways the one- and two-dimensional optical and HI rotation curves are derived. The one-dimensional optical rotation curves represent the rotation velocities measured along a slit aligned with the major axis, assuming inclinations based on optically determined axial ratios. In this respect they are derived in a similar fashion as the rotation curves of the galaxies in XV-Sample (Sect. 3).

In summary, obtaining rotation velocities from one-dimensional observations along the major axes of galaxies, either optically (Rubin et al. 1985, Mathewson et al. 1992) or in the radio wavelength regime (as described here, see Sect. 5), does not decrease the scatter in the TF relation significantly. It should be noted that the use of the random-motion corrected linewidths by using Eq.(??) with any of the random-motion parameters used in this paper, always fails to reproduce the slopes of the '$V_{\rm flat}$' or '$V_{\rm max}$' TF relations.

6. SUMMARY AND CONCLUSIONS

In the first part of this paper we have shown that it is possible to derive first-order rotation curves from the XV-maps. The main uncertainty in the derivation of these curves is the run of inclination angle with radius, since only information along one spatial direction is available. From each rotation curve a so-called representative rotation velocity is determined, which defines the 'best' estimate of the rotation velocity of a system.

A rotation velocity was also determined from the width of the global HI profile. This can be done, provided that corrections are applied for random gas motions. From the comparison of the global profile widths and the rotation velocities, obtained from kinematical fits to two-dimensional

velocity fields for a sample of 28 galaxies (RC-Sample), we found that the most-frequently used random-motion correction formulae (TFq) are not very satisfactory. For a large sample of galaxies the rotation velocity parameter ($W_{\rm R}^{\rm i}$), derived with these corrections, may be statistically equal to the true rotation velocity, but in individual cases the differences can be large, since one of the parameters in these correction formulae, the correction term for random gas motions $W_{{\rm t},l}$, varies considerably from galaxy to galaxy. We find that there is not only a large spread in the value of $W_{\rm t}$, but it also depends on the way the rotation velocity of a galaxy is defined: by the 'true' maximum rotation velocity or by the velocity of the flat part of the rotation curve. If the first definition is chosen, then $W_{\rm t,20} = 20 \pm 16$ km s^{-1} (mean and standard deviation from the mean) and $W_{\rm t,50} = 8 \pm 12$ km s^{-1}; with the second definition the values are $W_{\rm t,20} = 30 \pm 24$ km s^{-1} and $W_{\rm t,50} = 18 \pm 19$ km s^{-1} . In any case these values are much smaller than the ones derived by FBGP, but still comparable with the values used by BGPV (i.e. $W_{\rm t,20} = 38$ km s^{-1} and $W_{\rm t,50} = 14$ km s^{-1}).

In the last part of this paper the TF relations for RC- and XV-Samples are analysed. Recently, it has become clear that the scatter in this relation can be reduced considerably by using rotation velocities from velocity fields instead of velocities derived from global HI profile widths (e.g. Schommer et al. 1993, Verheijen 2001). We found a similar effect for the sample of galaxies with accurate HI rotation curves mentioned above (RC-Sample), and this motivated us to investigate whether we could also achieve a reduction in the dispersion in the TF relation of XV-Sample by using the representative velocities ($V_{\rm XV}$), determined directly from the 'one-dimensional' rotation curves. Unfortunately, this was not the case; the differences between the TF relations using $W_{\rm R}$ and $W_{\rm XV}$ are small. Apparently, the improvement in the accuracy of the velocity parameter in the TF relation is related to the use of two-dimensional velocity information, which allows one to determine the inclination of a galaxy kinematically. From the work by, amongst others, Rubin et al. (1985) and the study described here, we conclude that the derivation of rotation velocities from one-dimensional observations along major axes of galaxies (either with optical or radio telescopes), using inclinations derived from optical axis ratios, does not reduce the scatter in the TF relation.

ACKNOWLEDGEMENTS: We would like to thank T. S. van Albada for his stimulation to start this project and H. van Woerden for his comments on the manuscript. This work was supported by Korea Research Foundation Grant (KRF-2002-070-C00045).

REFERENCES

Aaronson, M., Huchra, J., & Mould, J. 1979, ApJ, 229, 1
Ashman, K. M. 1990, ApJ, 359, 15
Begeman, K. G. 1987, Ph.D. Thesis, University of Groningen
Begeman, K. G. 1989, A&A, 223, 47
Bosma, A. 1978, Ph.D. Thesis, University of Groningen
Bothun, G., Schommer, R., Williams, T., & Mould, J. 1992, ApJ, 388, 253
Bottema, R., Shostak, G. S., & van der Kruit, P. C. 1987, Nature, 328, 401
Bottinelli, L., Gouguenheim, L., Paturel, G., & de Vaucouleurs, G. 1983, A&A, 118, 4 (BGPV)
Bottinelli, L., Gouguenheim, L., Fouqué, P., & Paturel, G. 1990, A&AS, 82, 391
Broeils, A. H. 1992a, Ph.D. Thesis, University of Groningen
Broeils, A. H. 1992b, A&A, 256, 19
Broeils, A. H., & Rhee, M.-H. 1997, A&A, 324, 877
Broeils, A. H., & van Woerden, H. 1994, A&AS, 107, 129 (Paper I)
Capaccioli, M., Piotto, G., & Bresolin, F. 1992, AJ, 103, 1151

Carignan, C., & Beaulieu, S. 1989, ApJ, 347, 760
Carignan, C., & Freeman, K. C. 1985, ApJ, 294, 949
Carignan, C., & Puche, D. 1990a, AJ, 100, 394
Carignan, C., & Puche, D. 1990b, AJ, 100, 641
Carignan, C., Sancisi, R., & van Albada, T. S. 1988, AJ, 95, 37
Côté, S., Carignan, C., & Sancisi, R. 1991, AJ, 102, 904
Freedman, W. L., Hughes, S. M., Madore, B. F., Mould, J. R., Lee, M. G., Stetson, P., Kennicutt, R. C., Turner, A., Ferrarese, L., Ford, H., Graham, J. A., Hill, R., Hoessel, J. G., Huchra, J., & Illingworth, G. D. 1994, ApJ, 427, 628
Freedman, W. L., Lee, M. G., & Madore, B. F. 1996, private communication
Freedman, W. L., Madore, B. F., Hawley, S. L., Horowitz, I. K., Mould, J., Navarrete, M., & Sallmen, S. 1992, ApJ, 396, 80
Fouqué, P., Bottinelli, L., Gouguenheim, L., & Paturel, G. 1990, ApJ, 349, 1 (FBGP)
Giovanelli, R., Haynes, M. P., Salzer, J. J., Wegner, G., Da Costa, L. N., & Freudling, W. 1995, AJ, 119, 1059
Giraud, E. 1986, A&A, 174, 23
Jobin, M., & Carignan, C. 1990, AJ, 100, 648
Kelson, D. D., Illingworth, G. D., Freedman, W. L., Hill, R., Graham, J. A., Saha, A., Madore, B. F., Mould, J. R., Hughes, S. M. G., Stetson, P. B., Kennicutt, R. C., Ferrarese, L., Ford, H. C., Hoessel, J. G., & Huchra, J. 1994, BAAS, 26, 1352
Kolkman, O. 1995, private communication
Kraan-Korteweg, R. C. 1986, A&AS, 66, 255
Lake, G., Schommer, R. A., & van Gorkom, J. H. 1990, AJ, 99, 547
Madore, B. F., & Freedman, W. L. 1991, PASP, 103, 933
Martimbeau, N., & Carignan, C. 1994, AJ, 107, 543
Mathewson, D. S., Ford, V. L., & Buchhorn, M. 1992, ApJS, 81, 413
Pierce, M. J., & Tully, R. B. 1988, ApJ, 330, 579
Puche, D., Carignan, C., & Bosma, A. 1990, AJ, 100, 1468
Puche, D., Carignan, C., Wainscoat, R. J. 1991, AJ, 101, 447
Puche, D., Carignan, C., van Gorkom, J. H. 1991, AJ, 101, 456
Rhee, M.-H. 1996, Ph.D. Thesis, University of Groningen
Rhee, M.-H. 2004a, JKAS, 37, 15
Rhee, M.-H. 2004b, JKAS, 37, 91
Rhee, M.-H., & van Albada, T. S. 1996, A&AS, 115, 407 (Paper II)
Roberts, M. S. 1978, AJ, 83, 1026
Roelfsema, P. R., & Allen, R. J. 1985, A&A, 146, 213
Rubin, V. C., Burstein, D., Ford, W. K. Jr., Thonnard, N. 1985, ApJ, 289, 81
Sancisi, R., & Allen, R. J. 1979, A&A, 74, 73
Schommer, R., Bothun, G. D., Williams, T. B., & Mould, J. R. 1993, AJ, 105, 97
Tormen, G., & Burstein, D. 1995, ApJS, 96, 123
Tully, R. B. 1988, Nearby Galaxy Catalogue (Cambridge: Cambridge University Press) (NBG)
Tully, R. B., & Fisher, J. R. 1977, A&A, 54, 661
Tully, R. B., & Fouqué, P. 1985, ApJS, 58, 67 (TFq)
van Albada, T. S., Bahcall, J. N., Begeman, K. G., & Sancisi, R. 1985, ApJ, 295, 305
van Albada, T. S., & Sancisi, R. 1986, Phil. Trans. Roy. Soc. London, A320, 447
Verheijen, M. A. W. 1997, Ph.D. Thesis, University of Groningen
Verheijen, M. A. W. 2001, ApJ, 563, 694